ACS Publications 1155 Sixteenth Street N.W.
Most Trusted. Most Cited. Most Read. Washington, DC 20036

ACS Nano

An Integrated Multilevel Approach Unveils Complex Seed-Nanoparticle Interactions and Their Implications for Seed Priming

Elisa Cappetta[1•], Carmine Del Regno[1•], Marisa Conte[1], Christian Castro-Hinojosa[2], Susel Del Sol-Fernández[2], Chiara Vergata[3], Matteo Buti[4], Rossella Curcio[1], Anil Onder[1], Pierluigi Mazzei[1], Nicola Funicello[5], Salvatore De Pasquale[5], Mattia Terzaghi[6], Pasquale Del Gaudio[1], Antonietta Leone[1], Federico Martinelli[3], Maria Moros[2,7], and Alfredo Ambrosone[1]*

● These authors contributed equally

* Corresponding author: aambrosone@unisa.it

Affiliations
1 Department of Pharmacy, University of Salerno, 84084, Fisciano, Italy
2 Instituto de Nanociencia y Materiales de Aragón, INMA (CSIC-Universidad de Zaragoza), 50009, Zaragoza, Spain
3 Department of Biology, University of Florence, 50019 Sesto Fiorentino, Italy
4 Department of Agriculture, Food, Environmental and Forestry Sciences (DAGRI), University of Florence, 50019 Sesto Fiorentino, Italy
5 Department of Physics "E.R. Caianiello", University of Salerno, 84084, Fisciano, Italy
6 Department of Biosciences, Biotechnologies and Environment, University of Bari Aldo Moro, 70121 Bari, Italy
7 Centro de Investigación Biomédica en Red de Bioingeniería, Biomateriales y Nanomedicina (CIBER-BBN), Spain

Received: July 6, 2023
Revised: November 1, 2023
Accepted: November 1, 2023

Abstract: Nanotechnology has the potential to revolutionize agriculture with the introduction of engineered nanomaterials. However, their use is hindered by high cost, marginal knowledge of their interactions with plants, and unpredictable effects related to massive use in crop cultivation. Nanopriming is an innovative seed priming technology able to match economic, agronomic, and environmental needs in agriculture. The present study was focused on unveiling, by a multilevel integrated approach, undisclosed aspects of seed priming mediated by iron oxide magnetic nanoparticles in pepper seeds (Capsicum annuum), one of the most economically important crops worldwide. Inductively coupled plasma atomic emission mass spectrometry and scanning electron microscopy were used to quantify the MNP uptake and assess seed surface changes. Magnetic resonance imaging mapped the distribution of MNPs prevalently in the seed coat. The application of MNPs significantly enhanced the root and vegetative growth of pepper plants, whereas seed priming with equivalent Fe concentrations supplied as FeCl3 did not yield these positive effects. Finally, global gene expression by RNA sequencing identified more than 2,200 differentially expressed genes, most of them involved in plant developmental processes and defense mechanisms. Collectively, these data provide evidence on the link between structural seed changes and an extensive transcriptional reprogramming, which boosts the plant growth and primes the embryo to cope with environmental challenges that might occur during the subsequent developmental and growth stages.

Keywords: iron oxide magnetic nanoparticles, nanopriming, seed−nanoparticle interactions, RNA-seq, Capsicum annuum

Graphical abstract

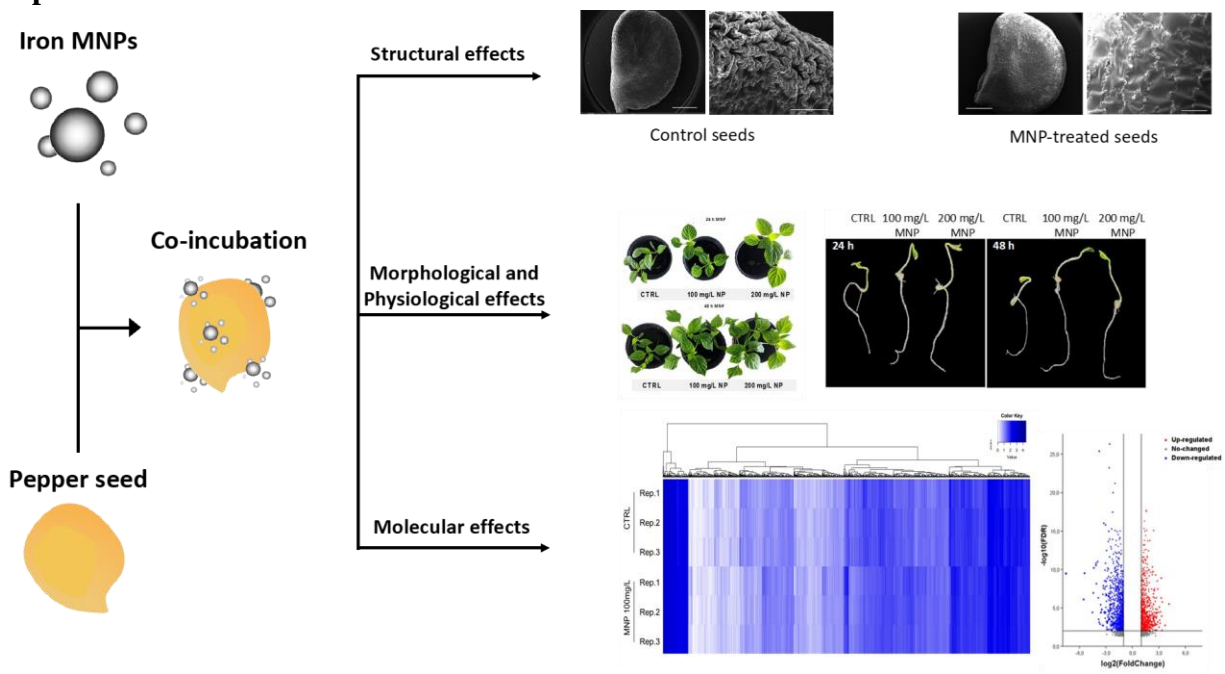

Introduction

Climate change, population growth, and the reduction of arable land pose significant threats to agriculture and undermine food security worldwide. Innovative actions are needed to overcome these constraints and ensure the sustainability and protection of major crops in the near future.1 Nanotechnology, if properly employed, has the potential to revolutionize the agricultural sector.

In the past decade, thanks to the small size and tailorable surface properties, engineered nanomaterials (NMs) have been used to overcome biological barriers in plants and to efficiently deliver micronutrients, antioxidants, and genetic materials, with the aim of improving plant productivity, resilience, and other agronomic traits.2−8

Furthermore, nanoenabled products can be used as components of smart sensors to advance the agronomic management of high-value crops.7,9

Irrespective of their different composition, the potential benefits of NM application in plant science and agriculture have not yet been fully exploited due to a limited understanding of biological interactions of nanoparticles with plants, including uptake, translocation, transformation, and bioavailability.10

High production costs and concerns about potential unpredictable environmental effects further restrict nanoenabled extensive farming.

In this scenario, seed nanopriming may be an opportunity to meet plant nanotechnology advances with economic and environmental needs. Basically, seed priming is a complex adaptive mechanism achieved through nonlethal exposure of seeds to biotic or abiotic stresses in a presowing stage. This process confers multiple advantages to the primed plants, including higher germination rates, vigorous development, enhanced nutrient utilization, and improved ability to respond to environmental constraints more quickly and robustly.11,12

Numerous successful strategies for seed priming have been described, including seed treatment with salt solutions (halo-priming), water (hydro-conditioning), osmotic agents (osmo-priming), plant hormone solutions (hormonal priming), exposure to high temperatures (heat priming), magnetic fields (magneto-priming), and, more recently, nanoparticles, known as seed nanopriming.13,14

Seed nanopriming technology is expected to minimize the input of NMs in agriculture, as low amounts of nanoparticles (NPs) can be used to pretreat thousands of small seeds, which are then washed to eliminate the excess of NPs that could be released into the environment. Seed nanopriming has been associated with enhanced germination rates, improved seedling growth, increased stress tolerance (such as drought or salinity), and better nutrient uptake in many crops.13,15

Nanopriming can also contribute to increase crop yields and overall plant health. Nonetheless, a substantial gap exists in our understanding of the physical interactions between seeds and NPs. Moreover, unraveling the regulatory networks responsive to nanoparticle stimuli holds the potential to elucidate their effects, mitigate undesired outcomes, and optimize the application of nanomaterials in agriculture. In this context, the use of magnetic iron oxide nanoparticles (MNPs) to prime plants has shown promise in boosting both growth and defense mechanisms in various plant species.16−18

However, the underlying mechanisms of these effects are still not fully understood.

In this study, we provide a comprehensive and multidisciplinary evaluation of MNP-mediated seed priming. Our goal was to gain a deeper understanding of how and to what extent MNPs influence seed germination and plant development using a range of analytical approaches including structural, physiological, phenotypic, and transcriptomic analyses.

The study was conducted in pepper (Capsicum annuum), one of the world's most economically and nutritionally important horticultural crops. We synthesized MNPs conjugated with a fluorophore (TAMRA) and tracked their internalization in the seeds using fluorescence microscopy. Analytic and imaging techniques, including Inductively Coupled Plasma Atomic Emission Spectroscopy (ICP-AES) and scanning electron microscopy (SEM), were used to quantify MNP internalization and to analyze surface structural modifications of the seeds.

Moreover, magnetic resonance imaging (MRI) was employed to create a map of MNP spatial distribution. We subsequently evaluated the impact of MNPs on embryo morphology and plant development, demonstrating their safety profile and positive influence on vegetative growth, not observed in plants primed with FeCl3, used as control to test the effects of the iron ionic counterpart. RNA sequencing revealed global gene expression changes induced by MNPs in pepper seeds. Considering the limited understanding of molecular impacts resulting from nanomaterial exposure in seeds, our approach contributes to gaining insights into the genetic aspects of plant nanobiotechnology. As a final remark, our data prove that MNP exposure modulates the expression of many biotic and abiotic stress-responsive genes, disclosing important implications for seed nanopriming.

Results And Discussion

MNP Synthesis and Characterization

Iron oxide MNPs are widely employed for various applications, owing to their exceptional properties. The established use of MNPs in the biomedical field as contrast agents for magnetic resonance imaging (MRI), drug delivery systems, and hyperthermia treatments for cancer has not revealed substantial hazards to human health. As a result, MNPs are now considered relatively safe.19−21 Moreover, the cost-effective synthesis of MNPs enables their application in agriculture, where they have been shown to have promising effects in augmenting crop production, enabling targeted delivery of agrochemicals and nutrients, enhancing plant development and resilience to different abiotic and biotic stress conditions, and ameliorating the decomposition of organic matter and the activities of microbial enzymes during the composting of agricultural waste.22−24

In this work, MNPs were synthesized by a one-step thermal decomposition method, obtaining MNPs coated with oleic acid soluble in organic solvents. These MNPs were transferred from hexane to water by coating them with an amphiphilic polymer poly(maleic anhydride-alt-1-octadecene) (PMAO) modified or not with tetramethylrhodamine-cadaverine (TAMRA), a fluorescent dye that facilitates MNP tracking (Figure 1a). MNPs@PMAO showed a mean diameter of 13.6 ± 2.9 nm, as determined from transmission electron microscopy (TEM) images (Figure 1b). The magnetization variation curve as a function of the applied magnetic field M (H) recorded at 300 and 5 K is shown in Figure 1c. At 300 K, the sample shows typical superparamagnetic behavior with negligible coercivity and remanence (see Table S1 in the Supporting Information). In contrast, the MNPs display a clear ferrimagnetic behavior at 5 K. Hydrodynamic diameter (Dh) and ζ-potential were determined with Malvern Zetasizer equipment, obtaining a size of 22.7 ± 0.9 nm and a surface charge of −48.0 ± 0.4 mV.

Although these MNPs are stable in aqueous media, they aggregate in more complex media due to the large number of carboxylic groups present on the PMAO surface. Thus, the MNP surface was passivated by functionalizing the polymer with α-methoxy-ω-amino polyethylene glycol (PEG, 5000 Da), increasing in this way their stability in more complex media.25

This step was performed by activating the carboxylic groups of the MNPs@PMAO with 1-ethyl-3-(3-dimethyl aminopropyl)carbodiimide (EDC) to bioconjugate the aminated PEG. The functionalization was evaluated by gel electrophoresis (agarose 1% w/v), evidencing a variation on the electrophoretic mobility promoted by the presence of PEG molecules (Figure S1).

Furthermore, an increment in the Dh to 45.9 ± 2.3 nm accompanied by a neutralization of the negative surface charge to −3 ± 0.4 mV was observed (Figure 1d,e), corroborating the functionalization of the MNPs@PMAO with PEG, named MNPs@PMAO@PEG5000. In addition, the successful PMAO coating and PEG coordination were confirmed by Fourier transform infrared (FT-IR) spectroscopy in MNP@PMAO and MNP@PMAO@PEG5000 samples (Figure S2). Surface Interactions and MNP Uptake in Pepper Seeds. While tangible progress has been made in understanding plant−NP interactions over the past decade, numerous challenges still need to be addressed before nanoenabled products can become widespread tools for studying and modulating plant functions. For instance, there is still a lack of understanding regarding the influence of NPs on seed structures and the mechanisms by which they enter the seeds, as well as the subsequent triggered biological effects.

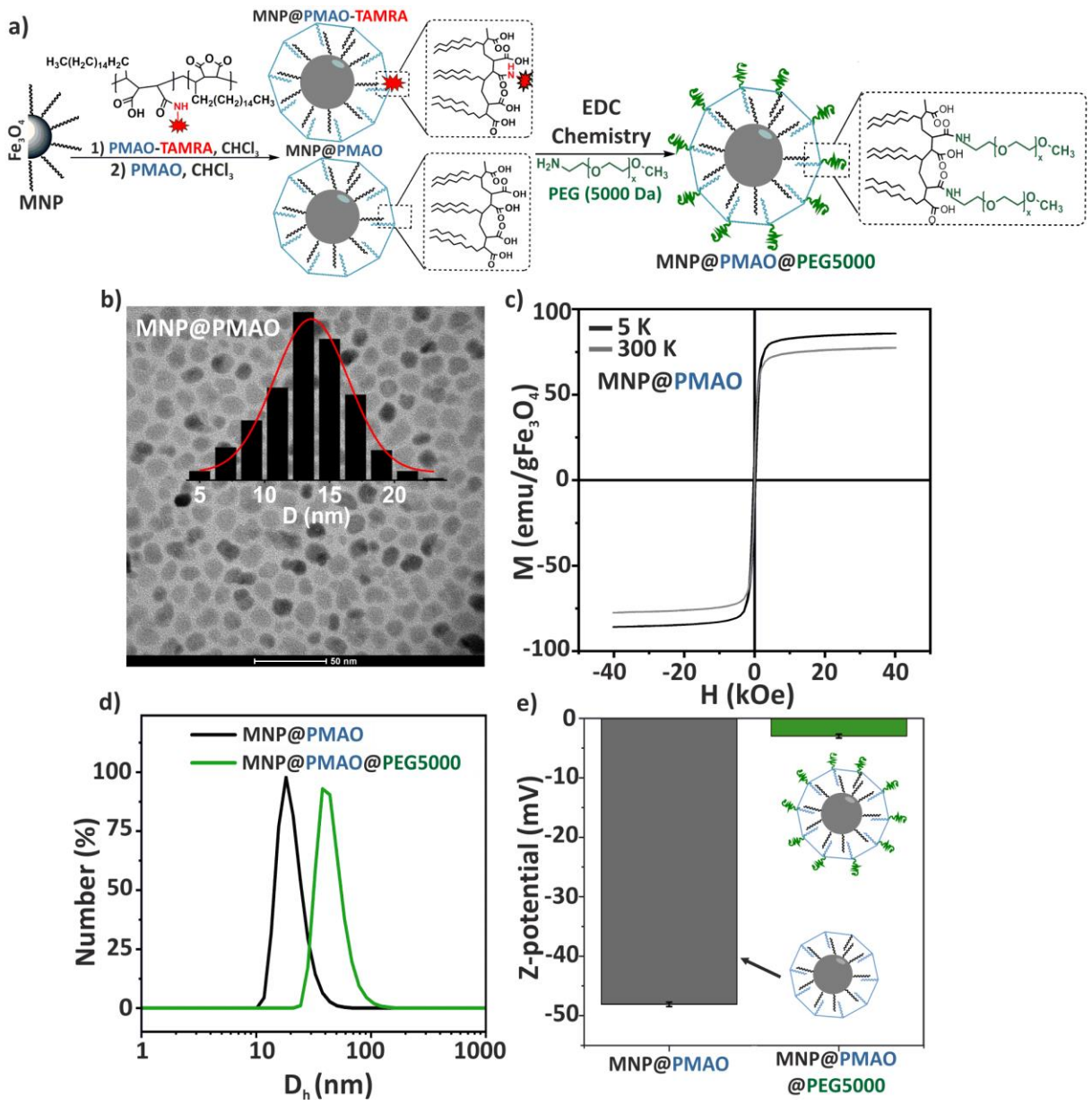

Figure 1. MNP synthesis and characterization. (a) Scheme of MNP transfer into water functionalization with PMAO or modified with TAMRA and functionalized with PEG (5000 Da) molecules by carbodiimide (EDC) chemistry. (b) TEM image of MNPs transferred to water and their size distribution. (c) Hysteresis loops recorded at 5 and 300 K. Inset: low-field hysteresis loops. (d) Hydrodynamic diameters measured by DLS and (e) ζ-potential measurements of MNPs@PMAO and after functionalization with PEG, MNPs@PMAO@PEG5000.

Surface Interactions and MNP Uptake in Pepper Seeds

In this study, we have utilized seeds of pepper, considering its significance as one of the most important horticultural crops. We initially used 100 mg/L of MNPs@PMAO@TAMRA@PEG to track the internalization of the MNP at the seed surface. After a 24 h incubation period, the seeds underwent thorough washing with distilled water to remove any MNPs that were not internalized. Subsequently, the seeds were dissected in order to separately image the tegument (Figure 2a−f) and the endosperm (Figure 2g−l). This examination revealed the presence of a diffuse staining pattern and numerous fluorescent spots on the outer layer of the seed coat (Figure 2e), which were not observed in the control seeds under the same microscope settings (Figure 2b). Additionally, a few fluorescent spots were detected within the

endosperm of the MNP-treated seeds (Figure 2k and l and Figure S3). These spots may indicate accumulations of MNPs, as generally observed in animal cells or tissues exposed to fluorescent NPs. These findings suggest that, following a 24-h exposure, the MNPs primarily localize in the seed coat of pepper seeds, with partial penetration observed in the endosperm. These results underline the potential implications for utilizing MNPs in the delivery of biomolecules into the seeds.

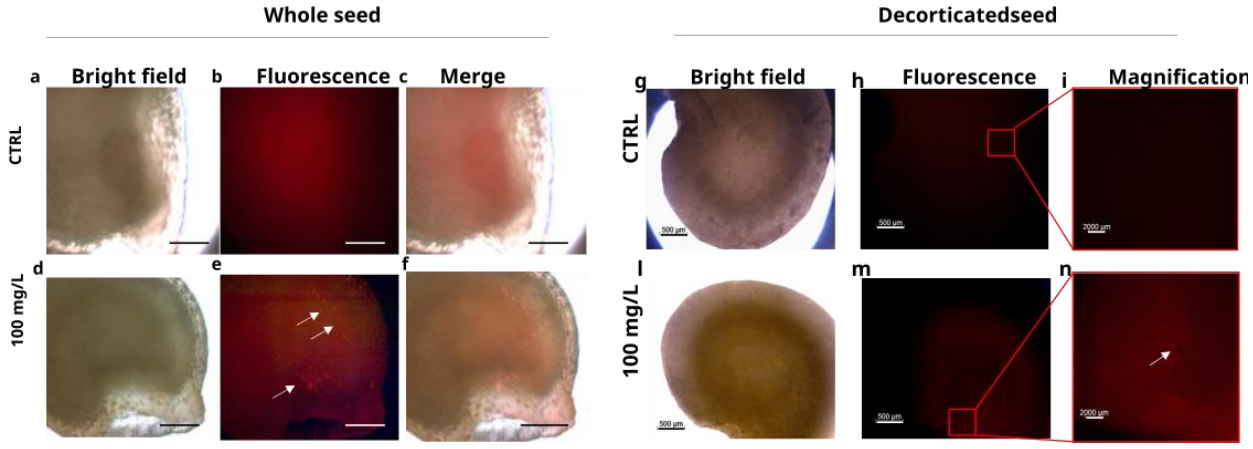

Figure 2. Fluorescence microscopy of C. annuum seeds treated with TAMRA-conjugated MNPs. (a) Bright field image of untreated seed. (b) Fluorescence imaging of a. (c) Overlap of (a) and (b). (d) Bright field image of a seed treated with 100 mg/L of NPs for 24 h. (e) Fluorescence imaging of (d). (f) Overlap of (d) and (e). (g) Decorticated control seed. (h) and (i) Fluorescence imaging of g at increasing magnification. (j) Seed treated with 100 mg/L of NPs for 24 h imaged after coat removal. (k) and (l) Fluorescence imaging of j at increasing magnification showing the presence of MNPs@PMAO@TAMRA@PEG in the endosperm. White arrows indicate MNP in the seed coat. Scale bars: 200 µm (left panel, a−f), 500 µm (g, h, j, k), and 2000 µm (i, l).

To quantitatively estimate the MNP internalization in the seeds, we determined the Fe content by ICP-AES analysis. To this aim, seeds treated with 100 and 200 mg/L of MNP@ PMAO@PEG for 24 h and untreated seeds were washed thoroughly, macerated in liquid nitrogen, and analyzed by ICPAES for the iron content determination which was 1.3 ± 0.6 µg/ seed in the control and 2.9 ± 0.5 µg/seed and 3.5 ± 0.8 µg/seed, respectively, upon treatments with 100 and 200 mg/L of MNPs.

To investigate further the structural effects of MNPs on seed coat, we performed a scanning electron microscopy (SEM) analysis after treating the seeds for 24 h with MNPs@PMAO@ PEG at two different concentrations. These observations showed that the tegument structure was drastically altered by the MNP exposure (Figure 3). In more detail, SEM micrographs revealed that the typical mesh-like structure of the control seed coat (Figure 3a−c) was modified upon 24 h exposure to 100 mg/L of MNP (Figure 3d−f) and 200 mg/L (Figure 3g−i), converting the tegument of MNP-treated seeds to a smooth and uniform surface rather than the typical wrinkled shape of control seeds kept for 24 h in MilliQ water. Previous studies have described a similar coat modification in Salvia leriifolia upon hydropriming.26

Although the biological significance of these structural changes of the seed coat is not fully understood, it is possible to hypothesize that the physical interactions between seeds and nanoparticles and consequent structural modifications might modify the coat permeability and likely the seed imbibition kinetics at an early stage of germination. Moreover, the structural modification might also contribute to the MNP internalization in the endosperm.

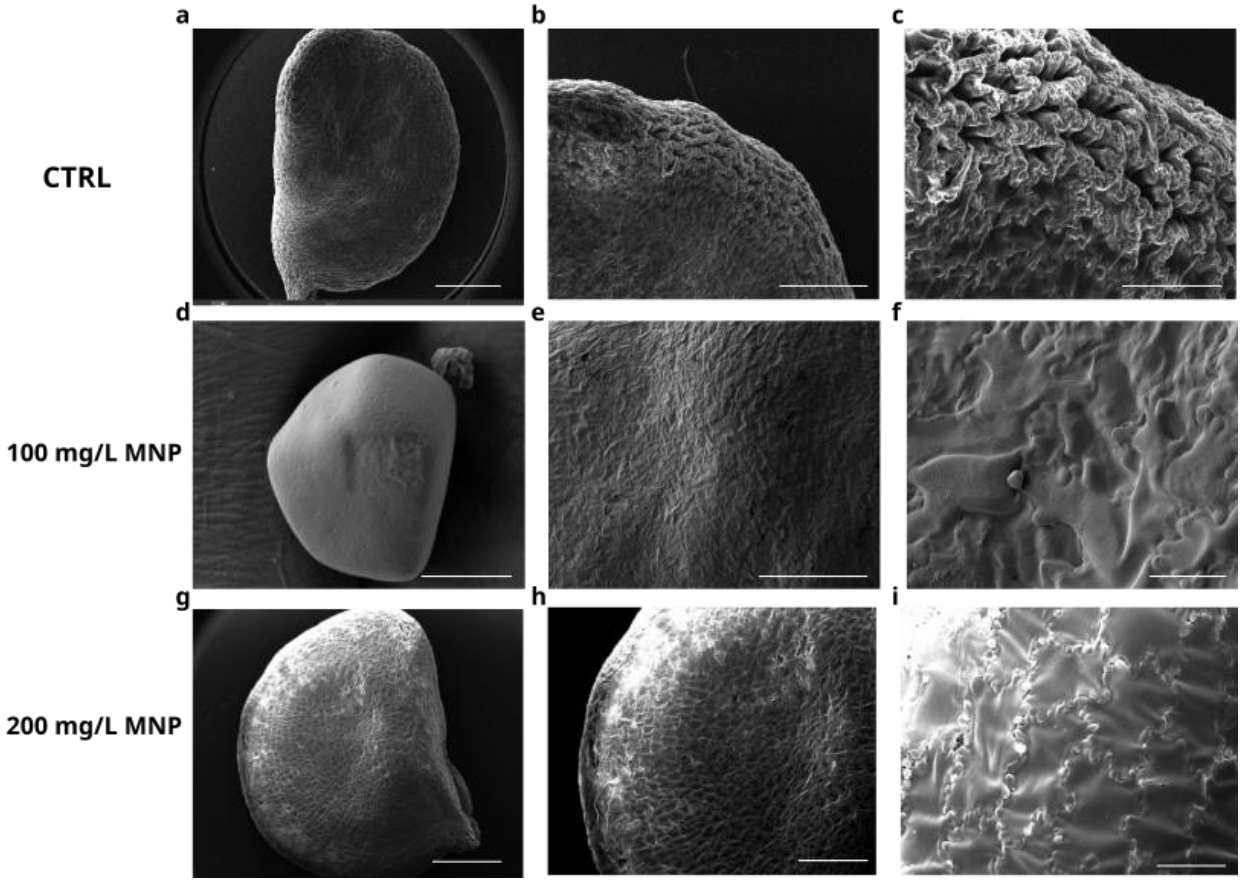

Figure 3. Scanning electron micrographs of untreated seeds (a−c) and seeds treated for 24 h with 100 mg/L of MNPs and (d−f) 200 mg/L of MNPs 200 mg/L (g, h, i). Scale bars: 1 mm in a, 500 μm in b, 200 μm in c, 2 mm in d, 500 μm in e, 50 μm in f, 1 mm in g, 500 μm in h, 100 μm in i.

NMR Imaging of Nanoprimed Seeds

To integrate the uptake study and profile the spatial distribution of MNPs in pepper seeds, nuclear magnetic resonance imaging (MRI) analysis was performed. 1 H MRI represents a noninvasive NMR spectroscopic technique capable of reconstructing images and revealing inner morphological characteristics of intact samples at a micrometer level. Proton MRI provides structural and conformational information based on amount, location, and mobility of water molecules.27,28

In this work, the MRI technique was used to prove and localize the presence of MNPs on seeds treated with 100 mg/L of MNPs. To this aim, pepper seeds were treated with MNPs@ PMAO@PEG, extensively washed, and dissected in order to analyze independently whole seeds, isolated teguments, and decorticated seeds. The disposition of whole seeds in the NMR tube is visible through a 3D reconstruction (Supporting Information, clip 1) and representative 2D axial slices (Figure S4). Representative spin density images of all samples are displayed in Figure 4 (upper panel, a−f).

Interestingly, although no significant difference in morphology emerged by a visual comparison between control and MNP-treated whole seeds, the spin density integrations revealed two types of profiles (Figure 4g and j), with a much lower response in the case of MNP-treated seeds and for the intensity histograms ranging within 115−135 (Figure 4j). The lower spin density integration values observed in the MNP-treated seeds may be likely attributed either to a lower content of water in examined seeds or to the presence of iron MNP, responsible for partially broadening and quenching proton signals.

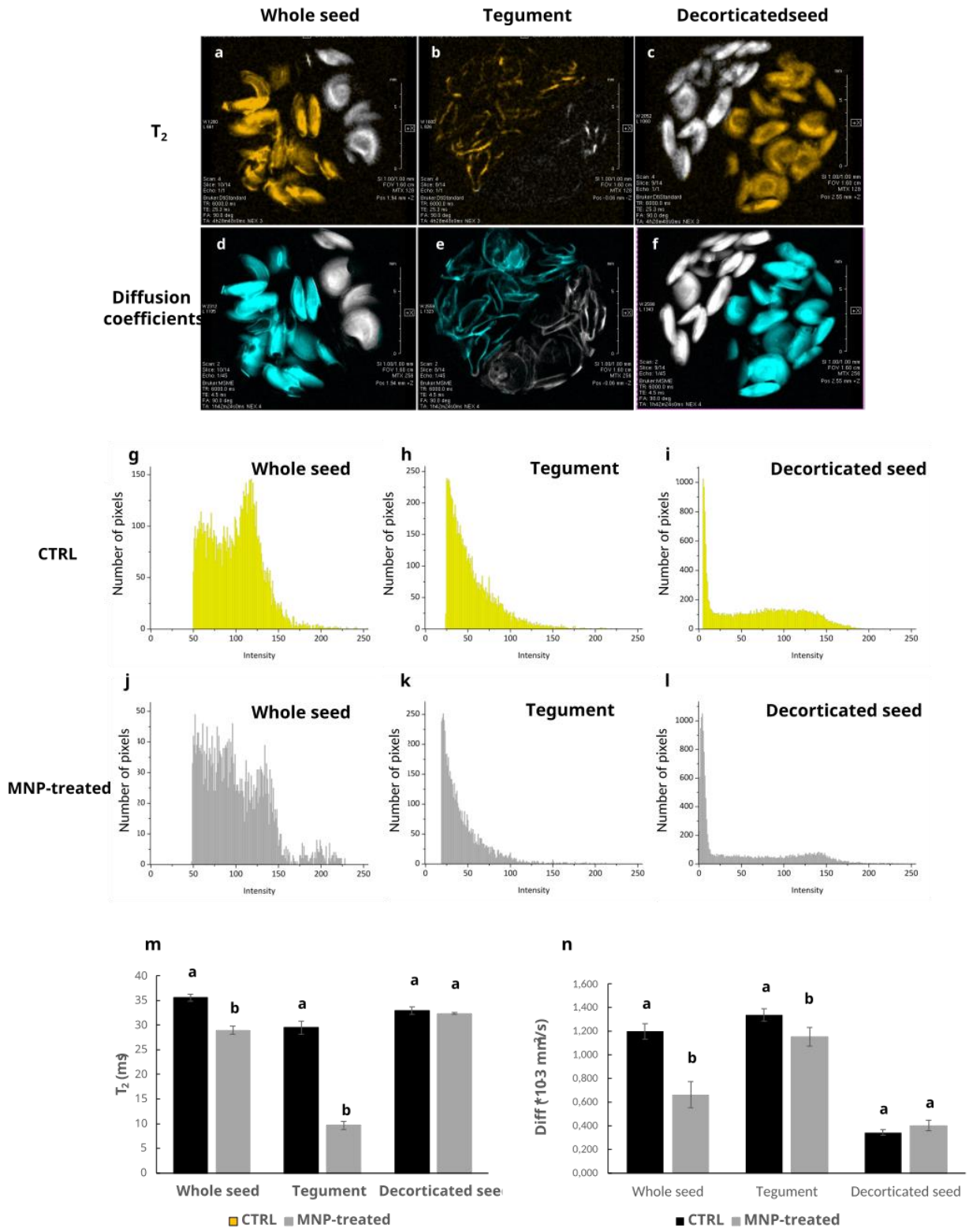

Figure 4. Upper Panel. Central axial slices for whole seed (a,d), tegument (b,e), and decorticated seed (c,f). The 3 images on the top are T2 experiments, while those on the bottom are diffusion experiments (yellow and cyan colors identify the control samples in T2 and Diff experiments, respectively). Central Panel. Spin density integrations (number of pixels per intensity) of axial slices of whole seed (g, j), tegument (h, k), and decorticated seed (i, l). The histograms on the top and bottom refer to control and MNP-treated samples, respectively. Bottom Panel. 1H NMR Spin−spin relaxation times (m) and self-diffusion coefficients (n) of whole seed, tegument, and decorticated seeds. Figures include, for each measure, the standard deviation, and the results of ANOVA

Tukey's test (0.05 confidence level and 95% of significance; letters a-b) on the histograms refer to the comparison between control and treated samples.

Afterward, an evaluation of the proton spin−spin relaxation time (T2) of the seeds was also conducted. Overall, a shortening of water proton T2 relaxation times is indicative of a change in the sample structure, at a nanoscopic level.29

Importantly, it is expected that MNP presence in seeds may strongly influence the nuclear chemical environment, by promoting and accelerating a faster T2 relaxation, due to the ferromagnetic nature of iron.30

Data reported in Figure 4m show that MNP-treated whole seeds exhibited a slightly lower T2 value with spin−spin relaxation times of 29 ms compared to 36 ms of control seeds.

The same evaluation was conducted on both the isolated teguments and the seeds deprived of tegument (decorticated seeds). While the spin−spin relaxation times in decorticated seeds resulted in constant and unaltered by MNP treatment, teguments exhibited a significant decrease in T2 values. In fact, the T2 relaxation was dramatically hastened in the isolated tegument of MNP-treated seeds, as compared to the isolated teguments of control seeds, since the values decreased from 29.5 to 9.7 ms (a 67% decrement). Accordingly, the T2 image of isolated teguments shown in Figure 4b revealed an almost total quenching of tegument signals in presence of MNPs. Such a variation is unequivocally due to the ferromagnetic action exerted by the iron contained in MNP. Altogether, these data provide clear evidence that MNPs were prevalently retained by the seed. Moreover, the low decrease in the T2 relaxation time of MNP-treated decorticated seeds compared to control untreated seeds confirmed that MNPs were mostly localized on the tegument.

The MNP-induced structural changes may affect the water dynamics in the seeds, and this possibility was evaluated by diffusion coefficients (DCs), which allow to estimate the apparent translational self-diffusion of water molecules within a plant tissue, thus indirectly estimating the extent of free diffusion within the studied matrix.31

Consequently, DCs are expected to decrease when water molecules experience barriers to diffusion, interact strictly with the matrix, or are forced to diffuse within relatively small-sized pores. Conversely, DC values increase if water molecules can move more freely into matrixes, characterized by longer free diffusion distance.28,32

DC values also proved to be very similar between control and MNP-treated decorticated seeds (Figure 4p). Conversely, a significant decrease of DC values was detected in the whole seeds and in the isolated teguments, indicating a slower mobility and a lower content of water at seeds' surface level. This might be the consequence of the adsorption of MNPs on the seed tegument surface, which restricts the retention of water on it and limits the penetration of water at the tegument−seed interface level, as shown in Figure 4n. Moreover, the decrease of tegument roughness revealed by SEM images in MNP-treated seeds suggests a decrease in cavities capable to retain water on the tegument surface, further contributing to lower diffusion coefficients at the surface level.

Interestingly, the latter aspect suggests that the difference was much more enhanced in the case of the whole seeds, as MNP-treated seeds received a lower penetration of water. In fact, in the case of control whole seeds, a larger amount of free-like water penetrated at the tegument−seed interface, thus implying a faster average diffusivity.

In summary, MRI experiments allowed us to prove the presence of MNPs on treated seeds and obtain indirect information on the tegument structural changes. In particular, T2 relaxation times suggested that

most of the MNPs were concentrated on the tegument. However, the internalization of a few MNPs in seed endosperm cannot be completely excluded, as also shown by fluorescence microscopy. On the other hand, diffusion experiments indicated that the water behavior and its penetration extent into the seed changed drastically, as a function of the treatment, especially at both the tegument and tegument−seed interface level.

MNP Effects on Embryo and Plant Development

We next investigated whether treatment with MNPs on pepper seeds might influence embryo and subsequent plant development. Quantitative measurements were conducted on the embryos by evaluating the diameter of the hypocotyl (HyD), the distance between root and shoot meristems (DRS), and the total embryo length (EL). As reported in Figure 5b, EL, DRS, and HyD did not show any significant changes in treated seeds compared to the control, indicating that the MNPs did not compromise the integrity of the pepper embryos.

To obtain an in-depth evaluation of nanopriming effects on pepper plant development, important physiological and morphological parameters, including germination, root length, leaf surface area, and chlorophyll index, were monitored in young plantlets from MNP-treated or control seeds.

Data reported in Figure 5c show that pepper seed germinability was unaffected by nanoparticle exposure, although a slight decrease in germination rate was observed in seeds after 72 h of priming with 200 mg/L of MNPs. Therefore, the analysis of other morpho-physiological parameters was conducted 24 and 48 h after nanopriming.

To evaluate the impact of MNPs on the seedling growth of C. annuum, we measured the root length of 14-day-old seedlings that were subjected to seed nanopriming at concentrations of 100 and 200 mg/L of MNP for 24 and 48 h. The results indicated a significant enhancement in relative root length after both 24 h of nanopriming, as depicted in Figure 5d−e. Notably, a 24 h nanopriming treatment led to an increase in root length of over 50% compared to the control seeds, as shown in Figure 5e.

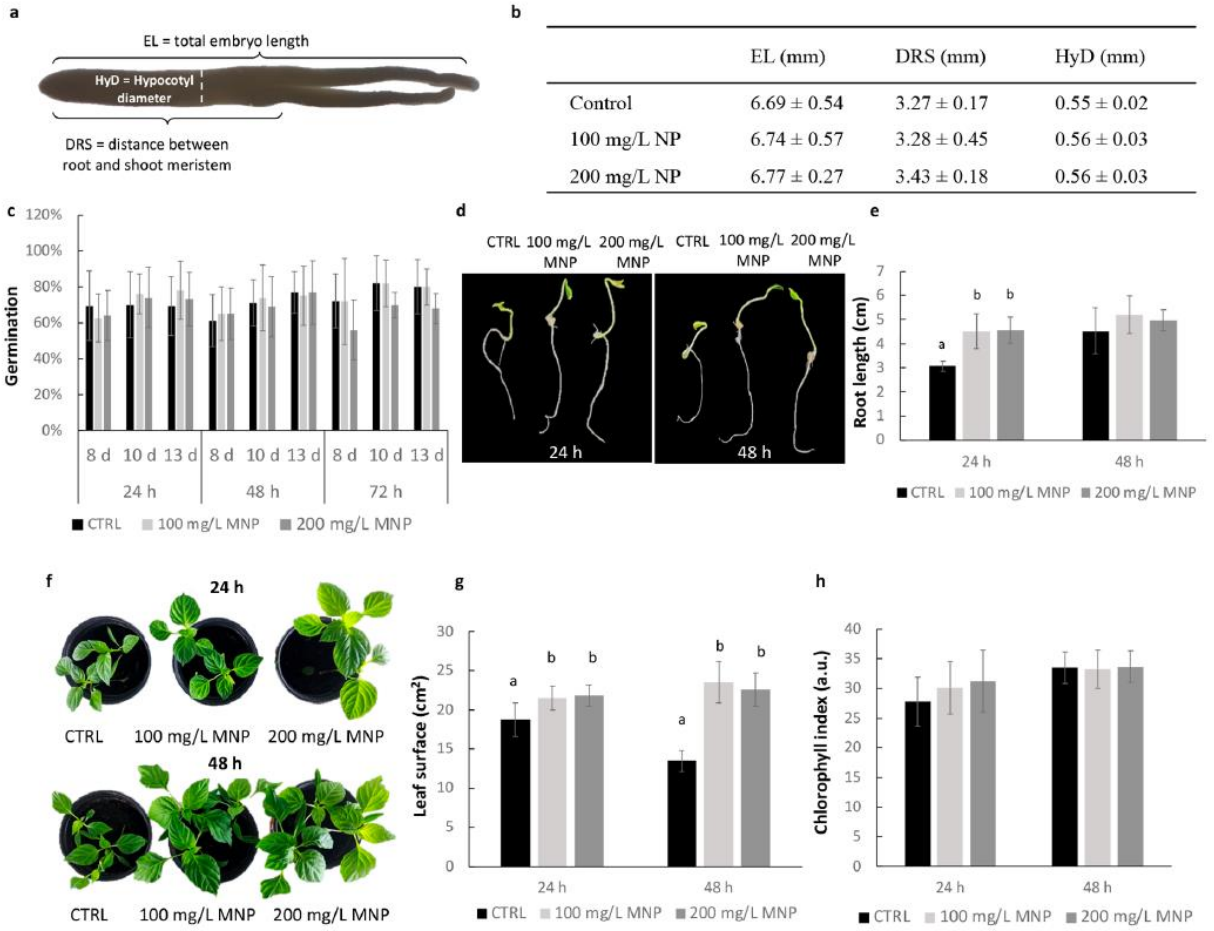

	EL (mm)	DRS (mm)	HyD (mm)
Control	6.69 ± 0.54	3.27 ± 0.17	0.55 ± 0.02
100 mg/L NP	6.74 ± 0.57	3.28 ± 0.45	0.56 ± 0.03
200 mg/L NP	6.77 ± 0.27	3.43 ± 0.18	0.56 ± 0.03

Figure 5. Physiological and morphological analyses after seed priming with MNPs. (a) Representative image of pepper embryos. (b) Morphometric analysis of pepper embryos after 24 h MNP exposure. EL, Total embryo length; DRS, Distance between root and shoot meristems; HyD, diameter of the hypocotyl. Values are means ± SD (n = 5). (c) Germination analysis of control and nanoprimed seeds. Seeds were treated with 100 and 200 mg/L of MNP for 24, 48, and 72 h, and germination data were collected after 8, 10, and 13 days. (d) Representative images of seedlings subjected to seed nanopriming with 100 mg/L and 200 mg/L of NP for 24 and 48 h. (e) Primary root length in control and nanoprimed seedlings. (f) Representative plants employed to determine leaf surface area. (g) Leaf surface area in control and MNP-treated plants. (h) SPAD measurements in control and MNP-treated plants to determine the chlorophyll index expressed as arbitrary units. The images and graphs shown are representative of at least three independent biological experiments. Statistical comparisons were performed using one-way ANOVA. The letters denote statistical significance with respect to untreated seeds ($P \leq 0.05$).

Afterward, the effects of seed nanopriming on vegetative growth were monitored by measuring leaf surface area, a key parameter directly linked to the quantity of light intercepted for photosynthesis, impacting plant growth and yield.33 Leaf areas of plantlets from control or nanoprimed seeds were measured 20 days after seedling transplanting. As reported in Figure 5g,h, seed nanopriming promotes a significant increase in leaf expansion in all treatments. Finally, we estimated the chlorophyll index of leaves which is commonly influenced by a variety of factors including nutrient availability and environmental stresses.34

Measurements by Soil Plant Analysis Development (SPAD) showed chlorophyll content values comparable to those of all treatment groups, indicating that MNP treatments did not significantly affect the chlorophyll levels in the leaves. Moreover, as SPAD values are commonly used as an indicator of leaf nitrogen status,35 our findings further support that MNPs did not have an impact on nitrogen content in

pepper plants. Finally, we compared the effects of MNPs to those of their iron ionic counterpart by priming the seeds with FeCl3. As reported in Figure S5, ionic iron did not produce significant effects on seed germination, root elongation, or leaf expansion after 48 h of exposure at both 100 and 200 mg/L Fe concentrations. Conversely, leaf expansion was negatively affected in plants primed for 24 h with 200 mg/L of Fe. These findings demonstrated that the influence of MNPs on plants diverges from that of their ionic counterpart, suggesting that growth-promoting effects cannot be solely attributed to the direct delivery of Fe ions by MNPs.

It is worth noting that the impact of seed nanopriming on physiology and development of pepper plants has been poorly investigated so far. However, a recent work reported that ZnO NPs applied to seeds inhibited seedling radical growth and promoted accumulation of phenolic compounds showing phytotoxic effects.36

Altogether, our data indicate that seed priming with iron oxide nanoparticles is able to stimulate root growth as well as to increase the plant vegetative growth in Capsicum annuum, confirming the stimulatory effects of nanoparticle-mediated seed priming already reported in different plant species.14,37,38

Therefore, as seed priming is a pivotal phase in seed preparation, focused on achieving optimal germination and early seedling establishment, the adoption of MNPs in this step may offer substantial benefits to seed companies and nurseries.

To better understand the underlying mechanisms of such a growth stimulation on plant growth of MNPs and to uncover their unexplored molecular effects, we also conducted a transcriptome analysis on pepper seeds exposed to MNPs.

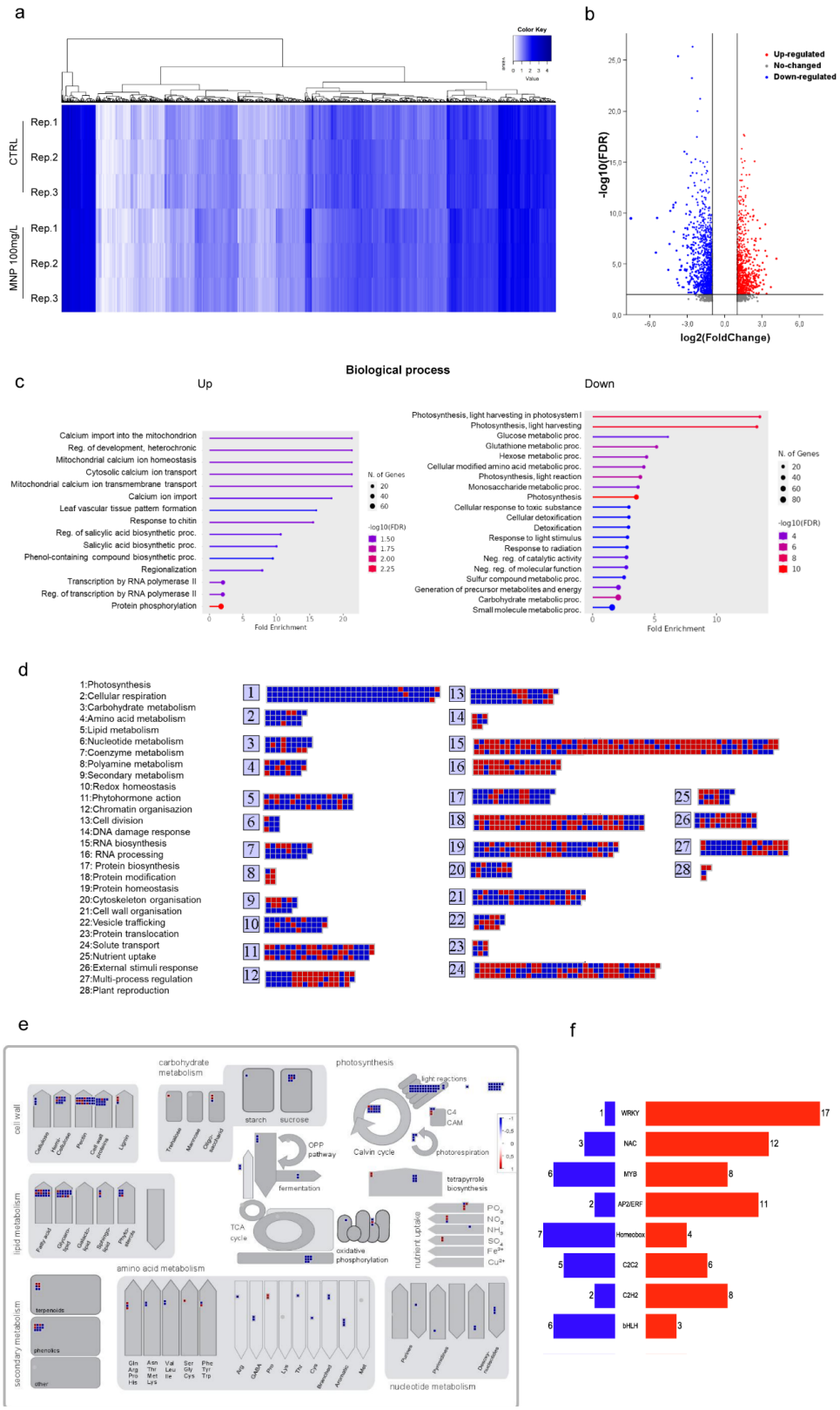

Figure 6. Transcriptome analysis of MNP-nanoprimed seeds. (a) Heatmap showing the expression levels in log10(FPKM + 1) of differentially expressed genes (FDR < 0.05, |log FC| > 1) upon MNP priming. (b) Volcano plot showing the differential gene expression in nanoprimed (100 mg/L) vs control (not treated) seeds. The data points above the significance threshold (FDR < 0.05, |log FC| > 1) are marked in blue (downregulated in 100 mg/L) and red (upregulated in 100 mg/L), and others are marked in gray (not significant). (c) GO biological process enrichment analysis (FDR < 0.05). (d) MapMan pathway (bin) representation

comparing up- (red) and down- (blue) regulated genes. (e) The "Metabolism overview" MapMan pathway employed to display expression changes of genes involved in primary and secondary metabolism upon exposure to 100 mg/L of MNP. (f) Identification and classification of the most abundant transcription factor families among the DEGs (red: upregulated; blue: downregulated).

Transcriptome Analysis in Nanoprimed Seeds

Overall, global gene expression analysis might reveal cellular responses to specific environmental challenges. There is a lack of knowledge regarding how nanoparticles affect the plant transcriptome.

Previous works have mostly concentrated on studying the effects of diverse nanoparticles, such as Ag NPs and Zn NPs, on adult plants in the model species Arabidopsis thaliana39 and tomato.40

In contrast, how priming with nanomaterials influences seed transcriptome has not yet been thoroughly investigated.

In this work, RNA sequencing (RNA-seq) was carried out to profile the transcriptomic changes associated with nanoparticle exposure in pepper seeds. Briefly, total RNA was extracted from seeds primed with 100 mg/L of MNP for 24 h and control seeds (hydroprimed). RNA sequencing generated 12−16 million raw read pairs per library, which were deposited in the EMBL-EBI ArrayExpress database under accession number E-MTAB- 13087. After trimming and filtering, 92−93% of read pairs remained, and 85−95% aligned to the ASM51225v2 reference genome (Table S2). Out of 35,845 predicted pepper transcripts, 18,395 were found active and used for subsequent analyses.

RNA library counts were normalized by their size, and multidimensional scaling (MDS) revealed clear separation between control and treated conditions (Figure S6). A differential expression analysis was carried out comparing the MNP-primed seeds and the control (hydroprimed) seeds (Figure 6a). We identified 2,204 differentially expressed genes (DEGs) in MNP-treated seeds (FDR $\leq$ 0.05), with 977 upregulated and 1,227 downregulated transcripts (Figure 6b and Supporting Information data set 1). Quantitative reverse transcription polymerase chain reaction (qRT-PCR) confirmed the expression patterns of 7 genes (4 upregulated and 3 downregulated). High consistency between the RNA-seq and RT-qPCR results was found using linear regression analysis of the fold change of gene abundance in treated versus control samples (R = 0.92, Figure S7), indicating that the data produced through RNA-seq are reliable. Conversely, the expression changes of selected genes observed via qRT-PCR in seeds exposed to FeCl3 were unrelated to those we observed by the RNA-seq analysis in MNP primed seeds (Figure S8), further proving that MNPs evoke a distinct biological response compared to the iron ionic counterpart.

Overall, we found that the molecular response of pepper seeds to MNPs involves an impressive higher number of genes with respect to those previously observed in adult plant tissues treated with different metallic and nonmetallic nanomaterials.39−42

These data suggest that, compared to treatments applied to adult plants, MNP-seed priming prompts a more extensive transcriptome reprogramming, which may prepare the embryo and the young seedling/plantlet to face unpredictable environmental conditions that might occur during the growth stages, optimizing the use of external resources and tuning their growth and development, accordingly.

In our study, the most upregulated genes in pepper seeds exposed to MNPs were C2H2-type domain-containing protein, ribosomal silencing factor RsfS, MLO-like protein, Pistil-specific extensin-like protein, interferon-related developmental regulator Nterminal domain-containing protein, WRKY domain-containing protein, and Brr2 N-terminal helicase PWI domain-containing protein. Conversely, among the most repressed transcripts, we found many genes involved in the photosynthesis such as

Chlorophyll a-b binding protein, photosystem I reaction center subunit N, and photosystem II reaction center X protein (Supporting Information data set 1).

To understand the potential biological significance of the extensive set of DEGs identified, we conducted a gene ontology (GO) enrichment analysis, focusing on the "biological process" (GO-BP) categories. Results displayed in Figure 6c show that the categories relative to calcium import, transport, and homeostasis were significantly enriched (FDR ≤ 0.05). Besides maintaining the intracellular homeostasis, Ca2+ acts as a key messenger in nutrient and stress signaling, as well as in plant development and immunity.43,44

This supports the notion that the activation of genes involved in calcium homeostasis and transport may be interconnected with the subsequent induction of gene sets involved in plant development and stress responses (e.g., response to chitin, response to salicylic acid) observed in nanoprimed seeds. A significant enrichment was found also for the GO-BP terms related to leaf vascular tissue formation, suggesting that MNP exposure might stimulate plant differentiation processes. Not least, the significant enrichment of GO terms related to the regulation of salicylic acid biosynthetic processes and phenol-containing compound biosynthetic processes points out a potential role of MNP priming in improving plants' defense mechanisms. We also observed that in the subset of upregulated genes "Transcription of RNA polymerase II", "Regulation of transcription by RNA polymerase II", and "Protein phosphorylation" were the most represented categories, which are likely responsible for the extensive remodeling of transcription and signaling processes required to cope with MNP exposure. By contrast, among the downregulated genes, we found a very strong enrichment of GO terms related to photosynthesis and other metabolic processes such as sugar and lipid metabolism (Figure 6c). Interestingly, a significant enrichment in downregulated genes was observed for categories related to cell detoxification. Consistent with the GO analysis, an analysis by MapMan software confirmed that downregulated genes were predominantly associated with pathways (bins) related to photosynthesis (PS I, PS II, Calvin cycle) and metabolic processes such as lipids (e.g., glycerolipids, fatty acids, and phytosterols), amino acids, sucrose metabolism, and tricarboxylic acid (TCA) cycle, as also schematized in the metabolism overview (Figure 6e).

The shutdown of this class of genes in a developmental embryo phase, depending exclusively on the seed storage substances, indicates that the cell energy may converge preferentially toward the transcriptional regulation of a network of genes related to plant defense. Interestingly, MapMan analysis also revealed a repression of many genes (e.g., pectinesterases, Alpha- and Betagalactosidases, GDSL esterases/lipases, and endoglucanases) known to be involved in cell wall organization. This is an important aspect as the cell wall is a frontline between the plant cell and the environment, and its structure and composition rapidly change when plants are subjected to biotic or abiotic stress.45

MapMan results also showed that several DEGs mapped in the Redox homeostasis pathway. In more detail, our analysis specifically identified 19 DE glutathione S-transferase (GST) genes, with 14 being downregulated and 5 upregulated. Concomitantly, MNPs are likely to downregulate expression of other genes known to be involved in the detoxification mechanisms such as the putative L-ascorbate peroxidase 3, peroxiredoxins, and thioredoxins.

Based on these data, it is reasonable to hypothesize that MNP treatment induces a mild nontoxic accumulation of ROS in seeds, as generally occurs in response to various factors, including water uptake during seed imbibition, seed priming, or exposure to different environmental stimuli. In this context, ROS are intended to act as signaling molecules that regulate seed germination, dormancy, and the growth of seedlings.46,47

It is important to note that the precise mechanisms through which MNPs induce ROS and the subsequent downstream effects require further investigation and elucidation.

Also, we found that the category related to solute transport exhibited a significant number of DEGs in treated seeds. In particular, calcium-permeable channel (OSCA) members serve as osmosensors in plants, enabling them to detect and react to both external and internal osmotic fluctuations. They play a crucial role in regulating plant growth and enhancing adaptability to environmental stressors.48,49

Not least, BIG and PIN, two key auxin transporters, were found to be upregulated in MNP-treated seeds. A previous study suggested that BIG may act synergistically with PIN1 to affect leaf growth.50 These data, together with the overexpression of genes involved in leaf vascular formation, may in part explain the positive influence of MNPs on the vegetative growth observed in young pepper seedlings and plantlets from primed seeds. Finally, MapMan analysis confirmed that upregulated genes were mostly involved in RNA biosynthesis and processing (including an impressive number of transcription factors), protein modification (e.g., phosphorylation), and chromatin organization processes (Figure 6d). A total of 152 transcription factors were differentially expressed in response to MNPs. Among them, 102 were found to be upregulated and 50 downregulated. Most of the TFs belong to the bHLH, C2H2, C2C2, WRKY, MYB, Homeobox, NAC, and ERF families (Figure 6f and Supporting Information Table S3). In particular, WRKY, ERF, and NAC TFs, mostly involved in plant development and abiotic stress responses,51,52 were prominently induced under MNP treatment, highlighting their potential pivotal role in managing the plant response to fluctuating external conditions in advanced growth stages.

To further understand the regulatory processes governed by the identified TFs in MNP-primed seeds, we constructed a protein−protein interaction (PPI) network using the STRING database (https://string-db.org/), based on the integration of various approaches, including experimental validation, text mining, databases, coexpression, and neighborhood interactions. Analyzing the downregulated TFs in the network, no significant connections or clusters were observed (Figure S9a). However, within the upregulated TFs, we identified a large cluster comprising 39 genes, including 15 WRKY, 6 AP2/ERF, and 5 NAC TFs, among others (Figure S9b and Supporting Information Table S4). This cluster exhibited strong relationships and enriched functional categories associated with the response to chitin, various stimuli, abiotic stress, as well as defense response and hormone-mediated signaling pathways such as salicylic acid (SA), jasmonic acid (JA), and ethylene (Figure S9c). These findings suggest that the use of nanoparticles could potentially induce a surge of hormone-mediated defensive responses. Accordingly, previous works have provided similar evidence, reporting that the application of NPs in plants can trigger defensive responses driven by increased levels of phytohormones (SA, JA, and abscisic acid) and the upregulation of genes involved in hormone-mediated defense signaling pathways.24,53−56

Conclusions

Herein, we showed that seed priming with MNPs is a safe technology and stimulates vegetative growth, an effect not observed in pepper seeds primed with $FeCl_3$. This underlines the significant impact of MNP physicochemical properties on exerting distinct biological effects with respect to the ionic counterpart during seed priming, a trend often described across various fields of application. Then, we also investigated at the molecular level how seeds respond to MNP treatment, reporting an extensive gene expression change. Nanopriming led to the suppression of photosynthesis-related genes and many energy pathways associated with ATP production. Moreover, MNP exposure downregulated genes encoding enzymes involved in the detoxification of ROS, suggesting that the maintenance of a sublethal level of ROS in germinating seeds may act as plant signaling molecules that participate in various plant growth

and developmental programmes. On the other hand, seed nanopriming enhances the expression of several genes encoding TFs known to regulate different defense pathways, indicating that the appropriate length and time of MNP exposure is sensed by plant cells as a sublethal stress-inducing event and triggers transcriptional changes that prime the embryo to better respond to external clues. Based on these results, we hypothesize that MNP-mediated priming may likely establish a somatic memory in primed plants that confers a greater ability to rapidly and effectively face unpredictable environmental changes that might occur during the following developmental stages. Many questions remain unanswered, including the duration of the priming effects which may vary based on plant genotypes, the potential involvement of epigenetic modifications, and the connection between MNP-induced transcriptional reprogramming and variations in seed hormonal homeostasis or ROS levels. The biotransformation of MNPs throughout various stages of plant development and their long-term effects on plant productivity are crucial aspects that demand comprehensive investigation, as well. These considerations are essential for gaining insights into the safety and sustainable utilization of MNPs in agriculture.

Not least, from a technological point of view, the results of this work have expanded the basic knowledge of the physical interaction between seeds and nanomaterials, providing valuable information for the MNP-mediated delivery of biomolecules (e.g., nucleic acids) into the seeds.

Methods

Synthesis and Functionalization of Iron Oxide Magnetic Nanoparticles. Magnetic nanoparticles (MNPs) were synthesized following a thermal decomposition method.57 Fe(III) acetylacetonate (15 mmol) was dissolved in dibenzyl ether (150 mL) in the presence of oleic acid (45 mmol) and 1,2-hexadecanediol (30 mmol) under a nitrogen flow and mechanic stirring. The mixture was heated to 200 °C and kept for 2 h. Then, the temperature was increased to reflux and kept for another 2 h. The mixture was cooled to room temperature under inert atmosphere, and the MNPs were washed with a mixture of hexane/ethanol four times, by magnetic separation.

To transfer the MNPs into water, 240 mg of poly(maleic anhydride-alt-1-octadecene) (PMAO) (MW: 30−50 kDa) was dissolved in a round-bottomed flask with 100 mL of $CHCl_3$ and MNP (10 mg of Fe) added dropwise.25

When fluorescent MNPs were needed, the polymer was previously modified with TAMRA as previously reported.58

The final mixture was sonicated for 15 min at room temperature, and thereafter $CHCl_3$ was evaporated using a rotary evaporator at 40 °C. In order to hydrolyze the anhydride groups present in the polymer and to confer stability in water to the MNPs, 30 mL of NaOH 0.05 N was added to the mixture, heated at 70 °C, and evaporated until reaching a final volume of 20 mL. The suspension was filtered using a Millipore filter (0.22 μm) to remove MNP aggregates, and the excess of polymer was eliminated by four consecutive ultracentrifugations at 70000g per 2 h each. The resultant nanoparticle suspension MNP@PMAO was stored at 4 °C. To functionalize the MNPs with PEG, MNPs (0.5 mg of Fe) previously coated with PMAO were mixed with 18.5 μmol of α-hydroxy-ω-amino PEG (MW: 5000 Da). Functionalization was carried out using 40 μmol of 1-ethyl-3-(3-dimethylaminopropyl)carbodiimide (EDC) in a borate-buffered saline (SSB) solution (50 mM, pH 9).25 The mixture was kept at 37 °C for 3 h. At that point, the MNPs were washed from the excess of reagents using ultracentrifugal filters (Amicon, Millipore, 100 kDa cutoff) and stored at 4 °C. Seed Nanoparticle Treatment. Pepper seeds (Capsicuum annuum, cv Friariello, TopSeed) were treated with 100 and 200 mg/ L of MNPs. Typically, 25 seeds were placed into a tube containing 1 mL of a given MNP suspension (Figure S10) and incubated on a rotator at room temperature in the dark

for 24, 48, or 72 h. Control seeds were kept in Milli-Q water and maintained as treated seeds (Figure S10). After the treatment, the seeds were surface sterilized using a 1% sodium hypochlorite solution for 2 min to prevent microbial contamination and then extensively rinsed in distilled water. Fe Quantification by Inductively Coupled Plasma Atomic Emission Spectroscopy (ICP-AES). To estimate the extent of MNP uptake, five seeds were incubated for 24 h with 100 mg/L or 200 mg/L of Fe supplied as MNPs, then washed, ground in liquid nitrogen, and digested with 250 μL of HNO3 (65% purity) and incubated during 2 h at 95 °C. After this time, 150 μL of HNO3 and 100 μL of H2O2 (33% w/ v) were added to the samples and digested overnight at 95 °C. Once digested, the samples were diluted up to a volume of 15 mL and were quantified by ICP-AES (Horiba Jobin Yvon) in duplicate and analyzed with the software Activa Analyst 5.4.

Fluorescence and Scanning Electron Microscopy

The internalization of MNPs@PMAO@TAMRA@PEG in pepper seeds was investigated by fluorescence microscopy (Axioplan 2, Zeiss).

Images were acquired with an Axiocam (Zeiss) camera and analyzed by Axiovision software (rel. 4.8, Zeiss). For scanning electron microscopy, three seeds for each treatment were extensively washed, fixed with 1 mL of 4% paraformaldehyde, and kept at 4 °C for 24 h. Seeds were spotted on carbon-coated electron microscopy grids. Samples were dried with nitrogen flux under a chemical fume hood. SEM images of the samples were then acquired using the Tescan S8000 microscope equipped with secondary electron and backscattered electron detectors (TESCAN s.r.o., Brno, CZ). Analyses were conducted at 1.5 and 5 keV without any coating of the particles, respectively. SEM images were taken from three independent experiments. Magnetic Resonance Imaging (MRI) of Pepper Seeds. All 1 H

MRI experiments were performed at 298 ± 1 K on a 300 MHz Bruker Avance wide-bore magnet (BrukerBiospin, Rheinstetten, Germany), equipped with a 1.5 mm μ-imaging MICRO 5 probe working at a 1 H frequency of 300.13 MHz. Seed samples were loaded into 15 mm sterilized NMR tubes (Norell − borosilicate). Treated and control seeds were loaded in the same NMR tube (at least 20 seeds per treatment) and examined concomitantly, to minimize any instrumental influence and emphasize possible evidence ascribable to the NP presence. In all cases, a rigid and transparent polypropylene layer (126 μm thick) was inserted into the tube to separate control from treated seeds, and a blue spongy and inert material with a semicircular shape was put to the tube bottom to easily recognize the tube side containing the control seeds (Figure S11). NMR tubes were tightly closed with a cap during the experimental acquisitions to limit the extent of water evaporation. Evaluation of Embryo Morphology. Under a stereomicroscope, the coat of treated and control seeds (five for each treatment) was removed by making a longitudinally shallow cut all around the seed with a razor blade. Secondary cuts were performed to free the embryo from the endosperm. Images of embryos were obtained under an optical microscope, and morphological traits (diameter of the hypocotyl, HyP; total length of the embryo, EL; distance between root and shoot apical meristems, DRS) were measured with ImageJ software. Germination Analysis and Plant Growth Measurements. Seeds were treated with 100 and 200 mg/L of MNPs and equivalent Fe concentrations supplied as salt (FeCl3) for 24, 48, and 72 h. After the treatments, the seeds were mildly surface-sterilized using a solution of sodium hypochlorite (0.45% NaOCl) and then placed in 10 cm Petri dishes on a filter paper (Whatman International Ltd., Maidstone, UK) and soaked in 2 mL of distilled water renewed every other day. The seeds were kept in the dark for 13 days at 23 °C in a growth chamber. Fifty seeds (10 seeds per plate) were sown for each treatment, and the percentage of germination was calculated. The data were collected over a period of 13 days post-treatment. Germination was evaluated as protrusion of the primary root. Germination tests were conducted in 5 independent biological experiments, each comprising 5 technical replicates.

To evaluate the root elongation after NP treatment, photographs of 13-day-old pepper seedlings grown on filter paper were taken and analyzed by the ImageJ software. For each treatment, the root length of ten seedlings was measured. Five independent experiments in technical triplicate were carried out. Leaf area was measured on plants 40 days after transplanting, using the ImageJ software to analyze the photographs of the displaced leaves on a white background. Chlorophyll Index. Four-week-old pepper plants were grown in pots containing universal soil (Triplo Natural Bio, TerComposti, Italy) in a growth chamber at 23 °C under a 16 h light/8 h dark photoperiod. Pepper plants of the same developmental stage were maintained in the condition of a regular water regime. Plants of the same developmental stage were maintained in condition of regular water regime. Soil Plant Analysis Development chlorophyll meter (SPAD, Minolta Camera Co., Osaka, Japan) was employed to determine the chlorophyll index. SPAD readings were taken at least in technical triplicate in five fully expanded upper leaves for each plant. At least three plants from each experimental condition were used in three independent experiments. RNA Extraction, Library Preparation, and Sequencing. Pepper seeds were incubated with 100 mg/L of MNPs and placed on a rotator at room temperature in the dark for 24 h. Control seeds were kept in Milli-Q water and maintained as treated seeds. After the treatment, seeds were rinsed in distilled water and placed in 10 cm Petri dishes on filter paper (Whatman International Ltd., Maidstone, UK) soaked in 2 mL of distilled water. After three days, total RNA was extracted from 10 seeds using 1 mL of TRIzol extraction buffer (Thermo Fisher Scientific, Wilmington, DE, United States) according to the manufacturer's protocol. RNA concentration was measured using a NanoDrop ND- 1000 spectrophotometer (Thermo Fisher Scientific, Wilmington, DE, United States). The RNA extracted from each sample was treated with DNaseI (NEB) and purified using a specific silica-based method following the manufacturer's instructions (Monarch RNA Cleanup kit − NEB). The quality of the processed extracts was assessed using a Bioanalyzer 2100 system (Kit RNA 6000 Nano - Agilent Technologies). A total of six extracts (three biological replicates for each treatment) were used for library preparation. Libraries were processed according to Illumina mRNA Library Prep kit instructions, and a dual index combination was used for each sample for barcoding. The concentration and quality of the libraries were evaluated using a Qubit 4 Fluorometer (dsDNA High Sensitivity Kit, Invitrogen) and Bioanalyzer 2100 system (HS DNA kit − Agilent Technologies). A sequencing was then run on the Illumina Novaseq6000 platform using a Novaseq 6000 S1 Reagent Kit (2 × 100 + 10 + 10 bp parameters). RNA-Seq Data Elaboration and Differential Expression analysis. The raw reads quality of the six RNA-Seq libraries was assessed using FastQC v0.11.9,59 while adaptor sequences and low quality bases were removed using Trimmomatic v0.3960 with these parameters: HEADCROP:1 LEADING:3 TRAILING:3 SLIDINGWINDOW:4:18 MINLEN:40. The filtered RNA reads of the six libraries were mapped to Capsicum annuum CM334 reference genome assembly ASM51225v261 downloaded from the Ensembl Plants Web site (https://plants.ensembl.org/, accessed on 08 March 2023). Reads counts were generated from the alignment files using featureCounts v2.0.362 with default parameters based on the "exon" feature and "transcript_id' meta-feature of Pepper Genome Annotation (PGA) gene predictions retrieved from the EnsemblPlants Web site (https:// plants.ensembl.org/, accessed on 08 March 2023).

Differential expression analyses were carried out using Bioconductor EdgeR v3.38.163 that was used to filter out the not expressed or poorly expressed transcripts (a transcript was considered "active" if reads per million mapping to that transcript was >1 in at least two RNA libraries), normalize the RNA libraries, and do the differential expression analysis between treated and control samples. The transcripts with resulting false discovery rate (FDR) lower than 0.05 and log 2(Fold Change) (LFC) lower than −1 or higher than 1 were considered as differentially expressed. Functional Annotation and Enrichment Pathway Analyses of DEGs. Gene ontology analysis was performed using ShinyGO V0.77 (Ge, S.X.; Jung, D.; Yao, R. Bioinformatics 2020, 36, 2628−2629) with a FDR cutoff 0.05. The MapMan software (version

3.5.1 R2)64 was used to annotate functional MapMan bin codes (BINs) of DEGs. The protein−protein interaction (PPI) profile of the 102 upregulated and 50 downregulated TFs was obtained from the STRING webserver (https://string-db.org/). To cluster the most similar nodes of the network into an easily distinguishable function-based classification, we employed the Markov Cluster Algorithm (MCL) for graphs. This is based on simulation of stochastic flow in the obtained graph. For achieving a balance between sensitivity and selectivity, we set the inflation factor at 1.1. Validation of Differentially Expressed Genes by Quantitative Polymerase Chain Reaction. Reverse transcribed DNase-treated total RNA (1 μg) was obtained using SuperScript III Reverse Transcriptase (Life Technologies, Carlsbad, CA, United States).

qRT-PCR was performed in a QuantStudio 5 Real-Time PCR Instrument. Each PCR reaction consisted of 1 μL of 1:20 diluted cDNA, 5 μL of 2X PowerUp SYBR Green Master Mix (Applied Biosystems, CA, United States), and 0.4 μM of each gene-specific primer in a total volume of 10 μL. All specific primer pairs were listed in Table S5. The thermal cycling conditions were 50 °C for 2 min (one step), one cycle at 95 °C for 2 min, followed by 40 cycles of two steps at 95 °C for 15 s, and 56 °C for 15 s. Three technical repetitions were performed for each sample. To normalize gene expression values, actin (AY572427) and glyceraldehyde-3-phosphate dehydrogenase (AJ246013) genes were used as internal control, whose expression upon MNP treatment was confirmed to be stable by RNA-seq.

Expression was calculated by the 2−ΔΔCT method.65

Expression levels of selected transcripts were measured in seeds primed with 100 mg/L of MNPs or with an equivalent Fe concentration supplied as FeCl3.

Control seeds were used as calibrator samples.

Statistics and Reproducibility

Sample size, number of replicates, and statistics tests for each experiment were described in the figure legends, where possible. Otherwise, these data were properly reported throughout the Methods section. Error bars in the graphical data represent standard deviations calculated on the mean of at least three independent experiments.

Associated Content

The Supporting Information is available free of charge at https://pubs.acs.org/doi/10.1021/acsnano.3c06172.

Additional data (images and tables) about MNP characterization, MNP internalization in seeds, MRI setup, physiological and morphological effects of seed priming with FeCl3, RNA-seq analyses, qRT-PCR analyses, and the list of primers (PDF) Movie of the disposition of all whole seeds in the NMR tube, appreciable through a 3D reconstruction (MOV) List of 2,204 differentially expressed genes (DEGs) in MNP-treated seeds (FDR ≤ 0.05), with 977 upregulated and 1,227 downregulated transcripts (XLSX)

Author Information

Corresponding Author Alfredo Ambrosone − Department of Pharmacy, University of Salerno, Fisciano 84084, Italy; orcid.org/0000-0002- 1897-4028; Email: aambrosone@unisa.it

Authors Elisa Cappetta − Department of Pharmacy, University of Salerno, Fisciano 84084, Italy Carmine Del Regno − Department of Pharmacy, University of Salerno, Fisciano 84084, Italy Marisa Conte − Department of Pharmacy, University of Salerno, Fisciano 84084, Italy Christian Castro-Hinojosa −

Instituto de Nanociencia y Materiales de Aragón, INMA (CSIC-Universidad de Zaragoza), Zaragoza 50009, Spain Susel Del Sol-Fernández − Instituto de Nanociencia y Materiales de Aragón, INMA (CSIC-Universidad de Zaragoza), Zaragoza 50009, Spain Chiara Vergata − Department of Biology, University of Florence, Sesto Fiorentino 50019, Italy Matteo Buti − Department of Agriculture, Food, Environmental and Forestry Sciences (DAGRI), University of Florence, Firenze 50144, Italy Rossella Curcio − Department of Pharmacy, University of Salerno, Fisciano 84084, Italy Anil Onder − Department of Pharmacy, University of Salerno, Fisciano 84084, Italy; orcid.org/0000-0002-7407-6409 Pierluigi Mazzei − Department of Pharmacy, University of Salerno, Fisciano 84084, Italy; orcid.org/0000-0002- 5312-4969 Nicola Funicello − Department of Physics 'E.R. Caianiello', University of Salerno, Fisciano 84084, Italy Salvatore De Pasquale − Department of Physics 'E.R. Caianiello', University of Salerno, Fisciano 84084, Italy Mattia Terzaghi − Department of Biosciences, Biotechnologies and Environment, University of Bari Aldo Moro, Bari 70121, Italy Pasquale Del Gaudio − Department of Pharmacy, University of Salerno, Fisciano 84084, Italy Antonietta Leone − Department of Pharmacy, University of Salerno, Fisciano 84084, Italy Federico Martinelli − Department of Biology, University of Florence, Sesto Fiorentino 50019, Italy Maria Moros − Instituto de Nanociencia y Materiales de Aragón, INMA (CSIC-Universidad de Zaragoza), Zaragoza 50009, Spain; Centro de Investigación Biomédica en Red de Bioingeniería, Biomateriales y Nanomedicina (CIBER-BBN), Madrid 28029, Spain; orcid.org/0000-0002-2861-2469 Complete contact information is available at: https://pubs.acs.org/10.1021/acsnano.3c06172

Notes The authors declare no competing financial interest.

Acknowledgments

We are grateful to Dr. Mina Formisano from TOPSEED Company (Sarno, Italy) who provided us the pepper seed selection. A.A. thanks the University of Salerno for financial support (FARB project). Part of the research activities were funded by the European Research Council (ERC) under the European Union's Horizon 2020 research and innovation programme granted to M.M. (Grant agreement No. 853468). M.M. also thanks MICIIN and FSE/Agencia Estatal de Investigación (Ramón y Cajal subprogram, grant RyC2019- 026860-I). A.O. is grateful to the Erasmus Traineeship Mobility.

References

(1) Wang, P.; Lombi, E.; Zhao, F. J.; Kopittke, P. M. Nanotechnology: A New Opportunity in Plant Sciences. Trends in Plant Science 2016, 21 (8), 699.

(2) Cohen, Y.; Yasuor, H.; Tworowski, D.; Fallik, E.; Poverenov, E.

Stimuli-Free Transcuticular Delivery of Zn Microelement Using Biopolymeric Nanovehicles: Experimental, Theoretical, and in Planta Studies. ACS Nano 2021, 15 (12), 19446.

(3) Ma, C.; Borgatta, J.; Hudson, B. G.; Tamijani, A. A.; De La TorreRoche, R.; Zuverza-Mena, N.; Shen, Y.; Elmer, W.; Xing, B.; Mason, S. E.; Hamers, R. J.; White, J. C. Advanced Material Modulation of Nutritional and Phytohormone Status Alleviates Damage from Soybean Sudden Death Syndrome. Nat Nanotechnol 2020, 15 (12), 1033.

(4) Kottegoda, N.; Sandaruwan, C.; Priyadarshana, G.; Siriwardhana, A.; Rathnayake, U. A.; Berugoda Arachchige, D. M.; Kumarasinghe, A. R.; Dahanayake, D.; Karunaratne, V.; Amaratunga, G. A. J. UreaHydroxyapatite Nanohybrids for Slow Release of Nitrogen. ACS Nano 2017, 11 (2), 1214.

(5) Zhao, L.; Lu, L.; Wang, A.; Zhang, H.; Huang, M.; Wu, H.; Xing, B.; Wang, Z.; Ji, R. Nano-Biotechnology in Agriculture: Use of Nanomaterials to Promote Plant Growth and Stress Tolerance. J. Agric. Food Chem. 2020, 68 (7), 1935.

(6) Wu, H.; Tito, N.; Giraldo, J. P. Anionic Cerium Oxide Nanoparticles Protect Plant Photosynthesis from Abiotic Stress by Scavenging Reactive Oxygen Species. ACS Nano 2017, 11 (11), 11283−11297.

(7) Giraldo, J. P.; Wu, H.; Newkirk, G. M.; Kruss, S. Nanobiotechnology Approaches for Engineering Smart Plant Sensors. Nature Nanotechnology 2019, 14, 541.

(8) Mittal, D.; Kaur, G.; Singh, P.; Yadav, K.; Ali, S. A. NanoparticleBased Sustainable Agriculture and Food Science: Recent Advances and Future Outlook. Frontiers in Nanotechnology 2020, DOI: 10.3389/fnano.2020.579954.

(9) Khater, M.; de la Escosura-Muñiz, A.; Merkoçi, A. Biosensors for Plant Pathogen Detection. Biosens Bioelectron 2017, 93, 72−86.

(10) Sanzari, I.; Leone, A.; Ambrosone, A. Nanotechnology in Plant Science: To Make a Long Story Short. Frontiers in Bioengineering and Biotechnology 2019, DOI: 10.3389/fbioe.2019.00120.

(11) Mauch-Mani, B.; Baccelli, I.; Luna, E.; Flors, V. Defense Priming: An Adaptive Part of Induced Resistance. Annu Rev Plant Biol 2017, 68, 485.

(12) Liu, H.; Able, A. J.; Able, J. A. Priming Crops for the Future: Rewiring Stress Memory. Trends in Plant Science 2022, 27 (7), 699.

(13) Nile, S. H.; Thiruvengadam, M.; Wang, Y.; Samynathan, R.; Shariati, M. A.; Rebezov, M.; Nile, A.; Sun, M.; Venkidasamy, B.; Xiao, J.; Kai, G. Nano-Priming as Emerging Seed Priming Technology for Sustainable AgricultureRecent Developments and Future Perspectives. J. Nanobiotechnol. 2022, DOI: 10.1186/s12951-022-01423-8.

(14) do Espirito Santo Pereira, A.; Caixeta Oliveira, H.; Fernandes Fraceto, L.; Santaella, C. Nanotechnology Potential in Seed Priming for Sustainable Agriculture. Nanomaterials 2021, 11 (2), 267.

(15) Imtiaz, H.; Shiraz, M.; Mir, A. R.; Siddiqui, H.; Hayat, S. NanoPriming Techniques for Plant Physio-Biochemistry and Stress Tolerance. Journal of Plant Growth Regulation 2023, 41, 6870.

(16) Waqas Mazhar, M.; Ishtiaq, M.; Maqbool, M.; Akram, R.; Shahid, A.; Shokralla, S.; Al-Ghobari, H.; Alataway, A.; Dewidar, A. Z.; ElSabrout, A. M.; Elansary, H. O. Seed Priming with Iron Oxide Nanoparticles Raises Biomass Production and Agronomic Profile of Water-Stressed Flax Plants. Agronomy 2022, 12 (5), 982.

(17) Moradbeygi, H.; Jamei, R.; Heidari, R.; Darvishzadeh, R.

Investigating the Enzymatic and Non-Enzymatic Antioxidant Defense by Applying Iron Oxide Nanoparticles in Dracocephalum Moldavica L. Plant under Salinity Stress. Sci Hortic 2020, 272, 109537.

(18) Abdoli, S.; Ghassemi-Golezani, K.; Alizadeh-Salteh, S. Responses of Ajowan (Trachyspermum Ammi L.) to Exogenous Salicylic Acid and Iron Oxide Nanoparticles under Salt Stress. Environmental Science and Pollution Research 2020, 27 (29), 36939.

(19) Materón, E. M.; Miyazaki, C. M.; Carr, O.; Joshi, N.; Picciani, P. H. S.; Dalmaschio, C. J.; Davis, F.; Shimizu, F. M. Magnetic Nanoparticles in Biomedical Applications: A Review. Applied Surface Science Advances 2021, 6, 100163.

(20) Moros, M.; Ambrosone, A.; Stepien, G.; Fabozzi, F.; Marchesano, V.; Castaldi, A.; Tino, A.; De La Fuente, J. M.; Tortiglione, C. Deciphering Intracellular Events Triggered by Mild Magnetic Hyperthermia in Vitro and in Vivo. Nanomedicine 2015, 10 (14), 2167.

(21) Mohsin, A.; Hussain, M. H.; Mohsin, M. Z.; Zaman, W. Q.; Aslam, M. S.; Shan, A.; Dai, Y.; Khan, I. M.; Niazi, S.; Zhuang, Y.; Guo, M. Recent Advances of Magnetic Nanomaterials for Bioimaging, Drug Delivery, and Cell Therapy. ACS Appl. Nano Mater. 2022, 5 (8), 10118.

(22) Spanos, A.; Athanasiou, K.; Ioannou, A.; Fotopoulos, V.; KrasiaChristoforou, T. Functionalized Magnetic Nanomaterials in Agricultural Applications. Nanomaterials 2021, 11 (11), 3106.

(23) Zhang, L.; Zhu, Y.; Zhang, J.; Zeng, G.; Dong, H.; Cao, W.; Fang, W.; Cheng, Y.; Wang, Y.; Ning, Q. Impacts of Iron Oxide Nanoparticles on Organic Matter Degradation and Microbial Enzyme Activities during Agricultural Waste Composting. Waste Management 2019, 95, 289.

(24) Kasote, D. M.; Lee, J. H. J.; Jayaprakasha, G. K.; Patil, B. S. Seed Priming with Iron Oxide Nanoparticles Modulate Antioxidant Potential and Defense-Linked Hormones in Watermelon Seedlings. ACS Sustain Chem Eng 2019, 7 (5), 5142.

(25) Moros, M.; Pelaz, B.; López-Larrubia, P.; García-Martin, M. L.; Grazú, V.; De La Fuente, J. M. Engineering Biofunctional Magnetic Nanoparticles for Biotechnological Applications. Nanoscale 2010, 2 (9), 1746.

(26) Ghodsimaab, S. P.; Makarian, H.; Ghasimi Hagh, Z.; Gholipoor, M. Scanning Electron Microscopy, Biochemical and Enzymatic Studies to Evaluate Hydro-Priming and Cold Plasma Treatment Effects on the Germination of Salvia Leriifolia Benth. Seeds. Front Plant Sci 2023, DOI: 10.3389/fpls.2022.1035296.

(27) Nuzzo, A.; Mazzei, P.; Savy, D.; Di Meo, V.; Piccolo, A. BioBased Hydrogels Composed of Humic Matter and Pectins of Different Degree of Methyl-Esterification. Molecules 2020, 25 (12), 2936.

(28) Mazzei, P.; Cozzolino, V.; Piccolo, A. High-Resolution MagicAngle-Spinning NMR and Magnetic Resonance Imaging Spectroscopies Distinguish Metabolome and Structural Properties of Maize Seeds from Plants Treated with Different Fertilizers and Arbuscular Mycorrhizal Fungi. J. Agric. Food Chem. 2018, 66 (11), 2580.

(29) Falcone, G.; Mazzei, P.; Piccolo, A.; Esposito, T.; Mencherini, T.; Aquino, R. P.; Del Gaudio, P.; Russo, P. Advanced Printable Hydrogels from Pre-Crosslinked Alginate as a New Tool in Semi Solid Extrusion 3D Printing Process. Carbohydr. Polym. 2022, 276, 118746.

(30) Marashdeh, M. W.; Ababneh, B.; Lemine, O. M.; Alsadig, A.; Omri, K.; El Mir, L.; Sulieman, A.; Mattar, E. The Significant Effect of Size and Concentrations of Iron Oxide Nanoparticles on Magnetic Resonance Imaging Contrast Enhancement. Results Phys 2019, 15, 102651.

(31) Price, W. S. Spin Dynamics: Basics of Nuclear Magnetic Resonance, 2nd Edition. Concepts in Magnetic Resonance Part A 2009, 34A (1), 60.

(32) van As, H.; Scheenen, T.; Vergeldt, F. J. MRI of Intact Plants.

Photosynthesis Research 2009, 102 (2−3), 213.

(33) Weraduwage, S. M.; Chen, J.; Anozie, F. C.; Morales, A.; Weise, S. E.; Sharkey, T. D. The Relationship between Leaf Area Growth and Biomass Accumulation in Arabidopsis Thaliana. Front Plant Sci 2015, DOI: 10.3389/fpls.2015.00167.

(34) Liu, C.; Liu, Y.; Lu, Y.; Liao, Y.; Nie, J.; Yuan, X.; Chen, F. Use of a Leaf Chlorophyll Content Index to Improve the Prediction of AboveGround Biomass and Productivity. PeerJ 2019, 6 (1), e6240.

(35) Xiong, D.; Chen, J.; Yu, T.; Gao, W.; Ling, X.; Li, Y.; Peng, S.; Huang, J. SPAD-Based Leaf Nitrogen Estimation Is Impacted by Environmental Factors and Crop Leaf Characteristics. Sci Rep 2015, DOI: 10.1038/srep13389.

(36) Garcia-Lopez, J.; Zavala-Garcia, F.; Olivares-Saenz, E.; LiraSaldivar, R.; Diaz Barriga-Castro, E.; Ruiz-Torres, N.; Ramos-Cortez, E.; Vazquez-Alvarado, R.; Nino-Medina, G. Zinc Oxide Nanoparticles Boosts Phenolic Compounds and Antioxidant Activity of Capsicum Annuum l. during Germination. Agronomy 2018, 8 (10), 215.

(37) Sun, H.; Qu, G.; Li, S.; Song, K.; Zhao, D.; Li, X.; Yang, P.; He, X.; Hu, T. Iron Nanoparticles Induced the Growth and Physio-Chemical Changes in Kobresia Capillifolia Seedlings. Plant Physiology and Biochemistry 2023, 194, 15.

(38) Hussian, I.; Ahmad, R.; Farooq, M.; Wahid, A. Seed Priming Improves the Performance of Poor Quality Wheat Seed under Drought Stress. Applied Science Reports 2014, DOI: 10.15192/ PSCP.ASR.2014.3.1.1218.

(39) Kaveh, R.; Li, Y. S.; Ranjbar, S.; Tehrani, R.; Brueck, C. L.; Van Aken, B. Changes in Arabidopsis Thaliana Gene Expression in Response to Silver Nanoparticles and Silver Ions. Environ. Sci. Technol. 2013, 47 (18), 10637.

(40) Sun, L.; Wang, Y.; Wang, R.; Wang, R.; Zhang, P.; Ju, Q.; Xu, J.

Physiological, Transcriptomic, and Metabolomic Analyses Reveal Zinc Oxide Nanoparticles Modulate Plant Growth in Tomato. Environ Sci Nano 2020, 7 (11), 3587.

(41) García-Sánchez, S.; Bernales, I.; Cristobal, S. Early Response to Nanoparticles in the Arabidopsis Transcriptome Compromises Plant Defence and Root-Hair Development through Salicylic Acid Signalling. BMC Genomics 2015, DOI: 10.1186/s12864-015-1530-4.

(42) Hong, J.; Jia, S.; Wang, C.; Li, Y.; He, F.; Gardea-Torresdey, J. L.

Transcriptome Reveals the Exposure Effects of CeO2 Nanoparticles on Pakchoi (Brassica Chinensis L.) Photosynthesis. J Hazard Mater 2023, 444, 130427.

(43) Yang, D. L.; Shi, Z.; Bao, Y.; Yan, J.; Yang, Z.; Yu, H.; Li, Y.; Gou, M.; Wang, S.; Zou, B.; Xu, D.; Ma, Z.; Kim, J.; Hua, J. Calcium Pumps and Interacting BON1 Protein Modulate Calcium Signature, Stomatal Closure, and Plant Immunity. Plant Physiol 2017, 175 (1), 424.

(44) Ghosh, S.; Bheri, M.; Bisht, D.; Pandey, G. K. Calcium Signaling and Transport Machinery: Potential for Development of Stress Tolerance in Plants. Current Plant Biology 2022, 29, 100235.

(45) Houston, K.; Tucker, M. R.; Chowdhury, J.; Shirley, N.; Little, A.

The Plant Cell Wall: A Complex and Dynamic Structure as Revealed by the Responses of Genes under Stress Conditions. Frontiers in Plant Science 2016, DOI: 10.3389/fpls.2016.00984.

(46) Bailly, C. The Signalling Roles of Reactive Oxygen Species in the Regulation of Seed Germination and Dormancy. Biochem. J. 2019, 476 (20), 3019.

(47) Farooq, M. A.; Zhang, X.; Zafar, M. M.; Ma, W.; Zhao, J. Roles of Reactive Oxygen Species and Mitochondria in Seed Germination. Frontiers in Plant Science 2021, DOI: 10.3389/fpls.2021.781734.

(48) Cao, L.; Zhang, P.; Lu, X.; Wang, G.; Wang, Z.; Zhang, Q.; Zhang, X.; Wei, X.; Mei, F.; Wei, L.; Wang, T. Systematic Analysis of the Maize OSCA Genes Revealing ZmOSCA Family Members Involved in Osmotic Stress and ZmOSCA2.4 Confers Enhanced Drought Tolerance in Transgenic Arabidopsis. Int J Mol Sci 2020, 21 (1), 351.

(49) Liu, C.; Wang, H.; Zhang, Y.; Cheng, H.; Hu, Z.; Pei, Z. M.; Li, Q.

Systematic Characterization of the OSCA Family Members in Soybean and Validation of Their Functions in Osmotic Stress. Int J Mol Sci 2022, 23 (18), 10570.

(50) Guo, X.; Lu, W.; Ma, Y.; Qin, Q.; Hou, S. The BIG Gene Is Required for Auxin-Mediated Organ Growth in Arabidopsis. Planta 2013, 237 (4), 1135.

(51) Nakashima, K.; Takasaki, H.; Mizoi, J.; Shinozaki, K.; Yamaguchi-Shinozaki, K. NAC Transcription Factors in Plant Abiotic Stress Responses. Biochimica et Biophysica Acta - Gene Regulatory Mechanisms 2012, 1819 (2), 97.

(52) Cappetta, E.; Andolfo, G.; Di Matteo, A.; Ercolano, M. R.

Empowering Crop Resilience to Environmental Multiple Stress through the Modulation of Key Response Components. J Plant Physiol 2020, 246−247, 153134.

(53) Khan, N.; Bano, A.; Ali, S.; Babar, M. A. Crosstalk amongst Phytohormones from Planta and PGPR under Biotic and Abiotic Stresses. Plant Growth Regulation 2020, 90, 189.

(54) Cai, L.; Cai, L.; Jia, H.; Liu, C.; Wang, D.; Sun, X. Foliar Exposure of Fe3O4 Nanoparticles on Nicotiana Benthamiana: Evidence for Nanoparticles Uptake, Plant Growth Promoter and Defense Response Elicitor against Plant Virus. J Hazard Mater 2020, 393, 122415.

(55) Shang, H.; Ma, C.; Li, C.; White, J. C.; Polubesova, T.; Chefetz, B.; Xing, B. Copper Sulfide Nanoparticles Suppress Gibberella Fujikuroi infection in Rice (Oryza Sativa L.) by Multiple Mechanisms: Contact-Mortality, Nutritional Modulation and Phytohormone Regulation. Environ Sci Nano 2020, 7 (9), 2632.

(56) Tripathi, D.; Singh, M.; Pandey-Rai, S. Crosstalk of Nanoparticles and Phytohormones Regulate Plant Growth and Metabolism under Abiotic and Biotic Stress. Plant Stress 2022, 6, 100107.

(57) Sun, S.; Zeng, H.; Robinson, D. B.; Raoux, S.; Rice, P. M.; Wang, S. X.; Li, G. Monodisperse MFe2O4 (M = Fe, Co, Mn) Nanoparticles. J. Am. Chem. Soc. 2004, 126 (1), 273.

(58) Moros, M.; Hernáez, B.; Garet, E.; Dias, J. T.; Sáez, B.; Grazú, V.; González-Fernández, Á.; Alonso, C.; De La Fuente, J. M. Monosaccharides versus PEG-Functionalized NPs: Influence in the Cellular Uptake. ACS Nano 2012, 6 (2), 1565.

(59) Andrews, S. Babraham Bioinformatics - FastQC A Quality Control tool for High Throughput Sequence Data. http://www.bioinformatics. babraham.ac.uk/projects/fastqc/. Last accessed 30 June 2023.

(60) Bolger, A. M.; Lohse, M.; Usadel, B. Trimmomatic: A Flexible Trimmer for Illumina Sequence Data. Bioinformatics 2014, 30 (15), 2114−2120.

(61) Kim, S.; Park, M.; Yeom, S. I.; Kim, Y. M.; Lee, J. M.; Lee, H. A.; Seo, E.; Choi, J.; Cheong, K.; Kim, K. T.; Jung, K.; Lee, G. W.; Oh, S. K.; Bae, C.; Kim, S. B.; Lee, H. Y.; Kim, S. Y.; Kim, M. S.; Kang, B. C.; Jo, Y. D.; Yang, H. B.; Jeong, H. J.; Kang, W. H.; Kwon, J. K.; Shin, C.; Lim, J. Y.; Park, J. H.; Huh, J. H.; Kim, J. S.; Kim, B. D.; Cohen, O.; Paran, I.; Suh, M. C.; Lee, S. B.; Kim, Y. K.; Shin, Y.; Noh, S. J.; Park, J.; Seo, Y. S.; Kwon, S. Y.; Kim, H. A.; Park, J. M.; Kim, H. J.; Choi, S. B.; Bosland,

P. W.; Reeves, G.; Jo, S. H.; Lee, B. W.; Cho, H. T.; Choi, H. S.; Lee, M. S.; Yu, Y.; Do Choi, Y.; Park, B. S.; Van Deynze, A.; Ashrafi, H.; Hill, T.; Kim, W. T.; Pai, H. S.; Ahn, H. K.; Yeam, I.; Giovannoni, J. J.; Rose, J. K. C.; Sørensen, I.; Lee, S. J.; Kim, R. W.; Choi, I. Y.; Choi, B. S.; Lim, J. S.; Lee, Y. H.; Choi, D. Genome Sequence of the Hot Pepper Provides Insights into the Evolution of Pungency in Capsicum Species. Nature Genetics 2014 46:3 2014, 46 (3), 270−278.

(62) Liao, Y.; Smyth, G. K.; Shi, W. FeatureCounts: An Efficient General Purpose Program for Assigning Sequence Reads to Genomic Features. Bioinformatics 2014, 30 (7), 923−930.

(63) Robinson, M. D.; McCarthy, D. J.; Smyth, G. K. EdgeR: A Bioconductor Package for Differential Expression Analysis of Digital Gene Expression Data. Bioinformatics 2010, 26 (1), 139−140.

(64) Thimm, O.; Bläsing, O.; Gibon, Y.; Nagel, A.; Meyer, S.; Krüger, P.; Selbig, J.; Müller, L. A.; Rhee, S. Y.; Stitt, M. MAPMAN: A User-Driven Tool to Display Genomics Data Sets onto Diagrams of Metabolic Pathways and Other Biological Processes. Plant Journal 2004, 37 (6), 914.

(65) Pfaffl, M. W. A New Mathematical Model for Relative Quantification in Real-Time RT-PCR. Nucleic Acids Res. 2001, 29 (9), 45e.